surfaces

MDPI

Article

Eco-Friendly Synthesis of Silver Nanoparticles Using Pulsed Plasma in Liquid: Effect of Surfactants

Yubiao Niu [1,*], Emil Omurzak [2], Rongsheng Cai [1], Dinara Syrgakbek kyzy [3], Zhanarbek Zhasnakunov [3], Abduraim Satyvaldiev [3] and Richard E. Palmer [1]

[1] Nanomaterials Lab, Mechanical Engineering, Swansea University, Bay Campus, Fabian Way, Swansea SA1 8EN, UK; rongsheng.cai@swansea.ac.uk (R.C.); r.e.palmer@swansea.ac.uk (R.E.P.)
[2] Department of Chemical Engineering, Faculty of Engineering, Kyrgyz-Turkish Manas University, Chyngyz Aitmatov Campus, Jal, Bishkek 720038, Kyrgyzstan; emil.omurzak@manas.edu.kg
[3] Faculty of Biology and Chemistry, Arabaev Kyrgyz State University, Bishkek 720026, Kyrgyzstan; diko.08@bk.ru (D.S.k.); janarbek@mail.ru (Z.Z.); satyvaldiev1948@mail.ru (A.S.)
* Correspondence: yubiao.niu@swansea.ac.uk

Abstract: Silver (Ag) nanoparticles were successfully prepared by using the in-liquid pulsed plasma technique. This method is based on a low voltage, pulsed spark discharge in a dielectric liquid. We explore the effect of the protecting ligands, specifically Cetyl Trimethylammonium Bromide (CTAB), Polyvinylpyrrolidone (PVP), and Sodium n-Dodecyl Sulphate (SDS), used as surfactant materials to prevent nanoparticle aggregation. The X-Ray Diffraction (XRD) patterns of the samples confirm the face-centered cubic crystalline structure of Ag nanoparticles with the presence of Ag_2O skin. Scanning Transmission Electron Microscopy (STEM) reveals that spherically shaped Ag nanoparticles with a diameter of 2.2 $\pm$ 0.8 nm were synthesised in aqueous solution with PVP surfactant. Similarly, silver nanoparticles with a peak diameter of 1.9 $\pm$ 0.4 nm were obtained with SDS surfactant. A broad size distribution was found in the case of CTAB surfactant.

Keywords: silver nanoparticles; pulsed plasma; ligand; surfactant

Citation: Niu, Y.; Omurzak, E.; Cai, R.; Syrgakbek kyzy, D.; Zhasnakunov, Z.; Satyvaldiev, A.; Palmer, R.E. Eco-Friendly Synthesis of Silver Nanoparticles Using Pulsed Plasma in Liquid: Effect of Surfactants. *Surfaces* **2022**, *5*, 202–208. https://doi.org/10.3390/surfaces5010013

Academic Editor: Mukhtar H. Ahmed

Received: 30 November 2021
Accepted: 14 February 2022
Published: 2 March 2022

1. Introduction

Many fields in both academia and industry are being revolutionised by the advancement of nanotechnology, due to its capability to tailor the properties of materials at the nanoscale [1]. Nano-sized metal particles (<100 nm) are of particular interest because of the growing opportunities in various fields, including sensing [2,3], catalysis [4–6], electronics [7,8] and optoelectronics [9,10], which arise from their special physical and chemical properties. Silver (Ag) nanoparticles are of special interest in this scenario [11]. One of the most important applications of Ag nanoparticles is as an antimicrobial agent against bacteria, fungi, and viruses [12–14]. Ag nanoparticles are safe and non-toxic to human and animal cells at low concentrations, and their toxicity in the environment is considered low compared with other materials [15]. Currently, many studies are being carried out to prepare advanced Ag-based antimicrobial agents [16]. For example, carbon-coated Ag particles are prepared to enhance stability, since carbon is biocompatible and has less of an effect on physiological conditions [17].

It is essential to take sustainability criteria into consideration across the full technology supply chain in the large-scale manufacturing and processing of nanomaterials [18,19]. Ag nanoparticles can be synthesised chemically and physically towards different targeted applications [20–25]. The chemical routes can provide good control of the size and morphology, but can involve toxic or costly precursors, solvents, and reductants [1]. On the other hand, the physical methods, such as magnetron sputtering, laser ablation, cluster beam deposition, and flame pyrolysis, can offer green routes to synthesise Ag nanoparticles, even if scale-up production can remain a challenge [26,27]. However, without the protection

of ligands, the physical methods tend to produce aggregates of nanoparticles with poor size control. Thus, a significant challenge is to prepare Ag nanoparticles in a simple and environmentally friendly way and, in particular, with well-controlled size and morphology.

Here, we report on a simple and promising method, the pulsed plasma in-liquid technique [28–30], to prepare Ag nanoparticles based on the electrical discharge between two Ag electrodes submerged in a dielectric liquid, which is believed to be ecologically friendly and cost-efficient compared with other traditional chemical methods [31]. By changing electrode materials and the dielectric liquid, this method is also capable of synthesising particles of other materials, such as metals, oxides, sulfides, carbides, etc. The physical and chemical properties can also be tuned by varying the experimental conditions, including sputtering potential and current [32]. During the preparation, different surfactant materials were added to the dielectric liquid to protect the synthesised nanoparticles from aggregation. XRD (XRD) and scanning transmission electron microscopy (STEM) were employed to investigate the composition and size distribution of the nanoparticles produced. The effects of the surfactant materials on the formation of the nanoparticles are reported here and discussed. This study opens a new way to stabilise metal nanoparticles synthesised on a large scale, with potential applications in biotechnology.

2. Materials and Methods

Pure Ag electrodes (2 mm in diameter and 10 mm in length) were submerged in a 50 mL pyrex beaker filled with deionised water. Plasma pulses (200 V, 50 A, 10 μs) were generated between the Ag electrodes for about 15 min. Several different surfactant materials have shown the best stabilizing properties for Ag nanoparticles, including the three ones studied in this work: Cetyl trimethylammonium bromide (CTAB) (molecular weight 364.45), Polyvinylpyrrolidone (PVP) (molecular weight 111.14n, average molecular weight 10,000), and Sodium n-Dodecyl Sulphate (SDS) (molecular weight 446.06). The surfactant materials were added to the water at 0.01 M concentration as stabilising agents to prevent nanoparticles from aggregating. The production yield of the samples has been found to depend on the melting point of the synthesised metals. For instance, low melting point metals, such as Zn and Sn, can usually be produced at a rate of up to a few grams per hour.

X-Ray diffraction (XRD) patterns of the samples were obtained using Cu Kα radiation, Rigaku RINT-2500VHF. The particle size distributions were characterised by a Thermo Fisher Scientific Talos Scanning Transmission Electron Microscope (STEM) with a convergence angle of 20 mrad and a high angle annular dark field (HAADF) detector operating with inner and outer angles of 62 mrad and 164 mrad at 200 kV. Samples were prepared by dispersing the nanoparticle powder in water and then drop-casting the suspension onto graphene oxide and holey carbon-coated copper grids.

3. Results and Discussion

Figure 1 shows the XRD patterns of the samples produced by the pulsed plasma in liquid between two Ag electrodes, with three different surfactant materials (SDS, CTAB, and PVP) and without any. Diffraction peaks corresponding to Ag and Ag_2O phases can be observed as labelled in Figure 1. The presence of Ag peaks confirms the successful synthesis of Ag nanoparticles. The Ag_2O results from the interaction of Ag nanoparticles with surfactant materials and other oxidising agents in the solution. The ratio of Ag/Ag_2O for each sample (weight percentages) was calculated from the integrated peak areas. The results are summarised in Table 1. The samples consist principally of two phases, Ag and Ag_2O, regardless of the type of surfactant. In addition, some other unknown peaks from impurities were also observed. The content of Ag nanoparticles formed in CTAB water solution was around 72.51%, which is slightly higher than that produced without any surfactant (Ag, 65.52%). In the case of samples produced with PVP, the composition (Ag, 64.62%) was very similar to that produced with pure water. The Ag nanoparticles formed in SDS water solution presented the smallest Ag ratio (43.94%). The cell crystal parameters

of Ag nanoparticles were also calculated, as summarised in Table 1. Although some small deviations (less than 1%) compared with the cell parameters from JCPDS card (No. 65-2871) were found, considering the use of surfactant materials and the dynamic conditions of the pulsed plasma in liquid, these deviations are small.

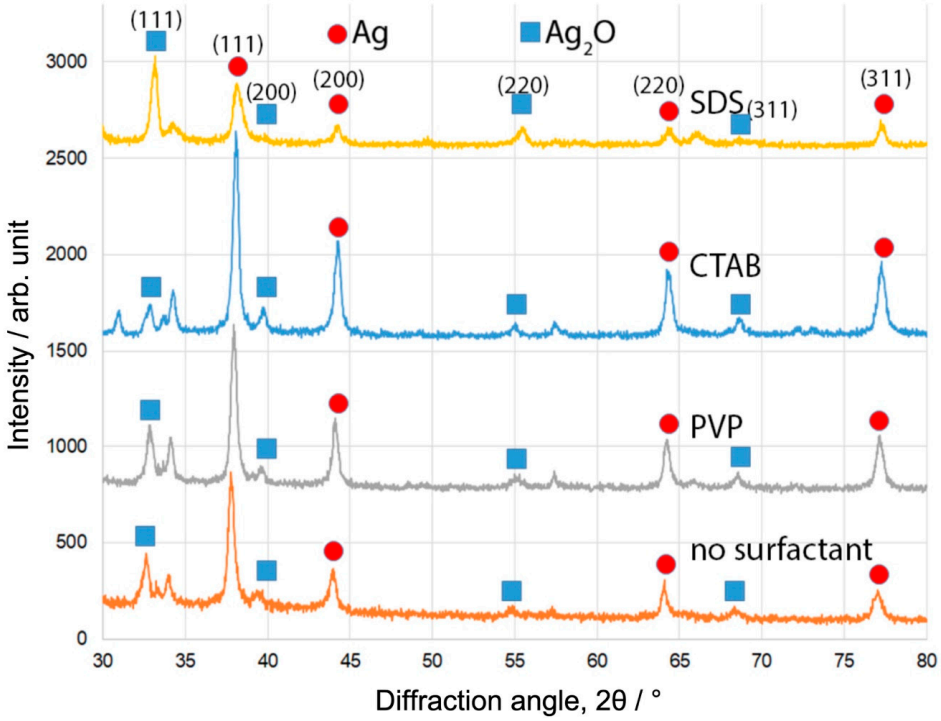

Figure 1. XRD patterns of Ag nanoparticles synthesised using pulsed plasma in aqueous solution in the presence of different surfactant materials. The individual peaks corresponding to different crystal planes from the Ag and Ag_2O phases are marked in the figure.

Table 1. Calculated content ratio of the constituent phases of the samples prepared using different kinds of surfactants and their cell parameters.

Samples	Constituent Phases (wt%)			Ag/Ag2O Ratio	Calculated Cell Parameters (Å)
	Ag	Ag_2O	Other		
SDS	43.94	43.87	12.19	1.00	4.0895
CTAB	72.51	16.75	10.74	4.33	4.0907
PVP	64.62	19.92	15.46	3.24	4.1007
no surfactant	65.52	20.29	14.19	3.23	4.1090
JCPDS #65-2871			/		4.086

Figure 2a shows typical HAADF-STEM images and size distribution of the Ag nanoparticles produced by the aqueous pulsed plasma technique in the presence of CTAB. Two peaks of cluster size in diameter are observed at 3.2 and 17.2 nm from its size distribution. The poor size distribution can be attributed to the weak interaction between Ag nanoparticles and CTAB. Figure 2b,c shows the STEM images and size distributions for Ag nanoparticles prepared with PVP and SDS, respectively. In contrast to the case of CTAB, the sizes distributions show single peak distributions for PVP and SDS, with diameters of 2.2 nm and 1.9 nm, respectively. This indicates PVP and SDS have stronger interaction with Ag than that of CTAB, which can protect Ag nanoparticles from growing into bigger ones more efficiently.

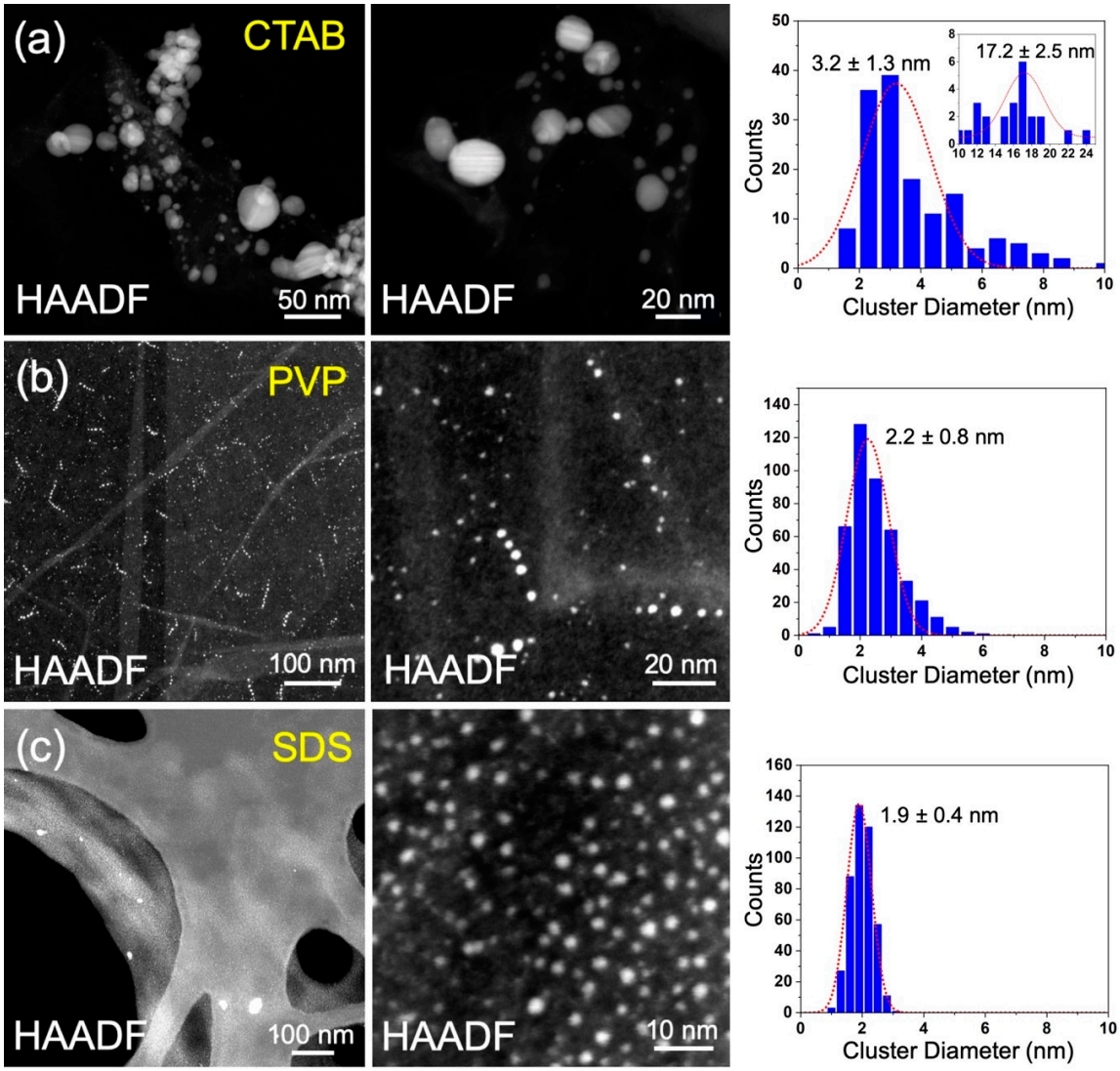

Figure 2. Typical HAADF-STEM images and size distributions for the Ag nanoparticles prepared using the aqueous pulsed plasma technique in the presence of CTAB (**a**), PVP (**b**), and SDS (**c**).

Figure 3a–c shows the energy dispersive X-ray spectroscopy (EDS) mapping of Ag nanoparticles prepared with CTAB. It confirms again the successful synthesis of Ag nanoparticles for both big and small sizes. The dominant element of the Ag nanoparticles is Ag, with a much higher signal to background ratio that that of element O. This can also be confirmed from the line profile of the elemental fraction (at.%) of the individual Ag nanoparticle shown in Figure 3d,e. The bulk of the Ag nanoparticle mainly consists of Ag. The ratio of Ag/O decreases quickly at the edge of the nanoparticles. This implies the presence an oxide layer on the surface of the Ag nanoparticle. The high-resolution TEM (HRTEM) image in Figure 3f shows the crystalline structure of the big Ag nanoparticles synthesised in CTAB solution. The FFT pattern (Figure 3g) of the boxed area in Figure 3f confirms the presence of both Ag(111) (d = 0.23 nm) and Ag_2O(111) (d = 0.27 nm) [33]. The contrast of the spots of Ag and Ag_2O implies that metallic Ag is dominant in the nanoparticles, with only a thin skin of Ag_2O having formed on the surface of Ag nanoparticles. This is in line with the XRD data and EDS data. It can be seen that the ratio of Ag/Ag_2O (Table 1) increases with the increase of the size of Ag nanoparticle. The smaller Ag nanoparticles shown in the cases of PVP and SDS hold larger surface to bulk ratio than that of the case of CTAB; they provide a significant amount of surface Ag atoms to be oxidised into Ag_2O.

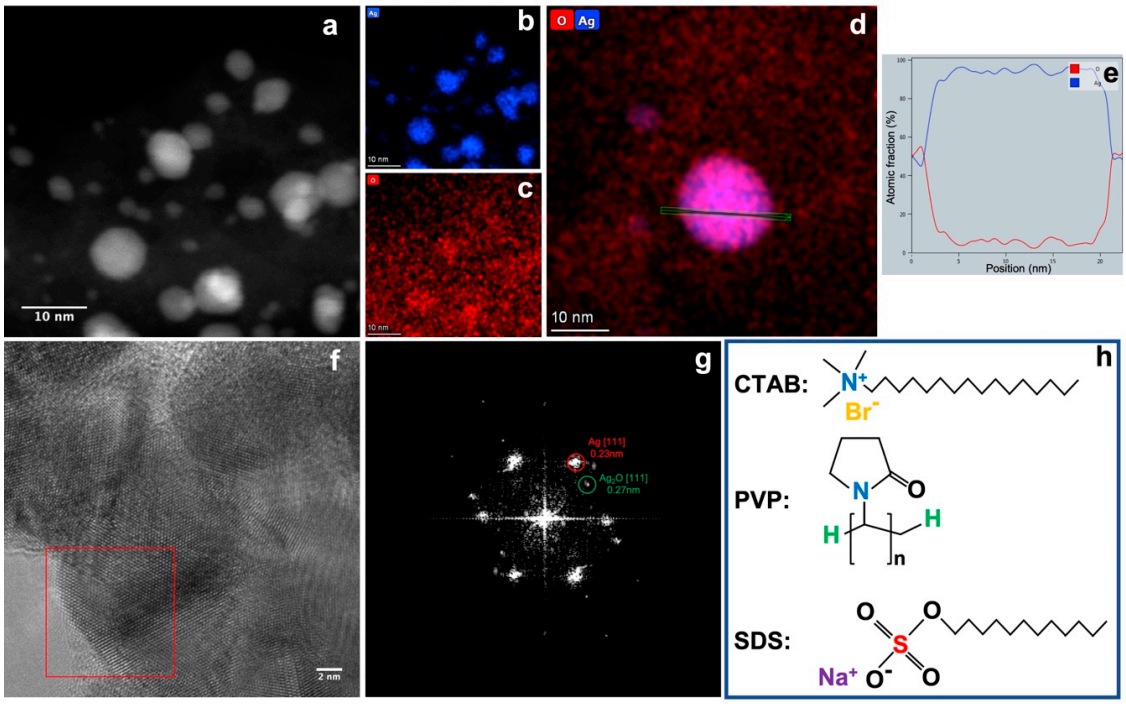

Figure 3. STEM image of Ag nanoparticles prepared with CTAB (**a**) and its EDS mappings of elements Ag (**b**) and O (**c**). EDS mapping of an individual Ag nanoparticle (**d**) shows the line profile (**e**) of the atomic fraction of Ag and O of the area marked in green in (**d**). HRTEM of Ag nanoparticles prepared with CTAB (**f**) and the FFT pattern of the nanoparticle boxed in red showing the presence of both Ag and Ag_2O (**g**,**h**) illustrates the chemical structures of the three kinds of surfactant.

Based on the XRD analyses, STEM observations, and relevant pieces of literature [34–38], the formation mechanism of the Ag nanoparticles and the Ag_2O skin can be proposed as below. The sputtered Ag ions/atoms in the hot plasma are quickly quenched by the surrounding liquid, aggregating with each other to form metallic Ag nanoparticles. Then, those Ag nanoparticles will react with the surfactant materials and O, OH, and H radicals dissociated from the water molecules due to the high temperature of the plasma. The dissolution of organic molecules introduced by hot plasma may take place, but it occurs only inside a tiny zone where the hot plasma is generated. Given that the duration of the electrical discharge is less than 10 µs and the gap between the two electrodes is less than 0.5 mm, the effect of the dissolution of organic molecules is negligible. As we know, there are many combinations between Ag and O, OH, H radicals [39]; thus, other metastable phases of Ag/O or Ag/OH can also be formed. Under the pulsed plasma in liquid conditions, hydroxide of silver is formed first, which immediately turns into an oxide. In this study, only Ag and Ag_2O phases were observed in the final product according to the XRD analysis. The structures of the three types of surfactant materials are shown in Figure 3h. Both PVP and SDS have oxygen groups which can strongly interact with the Ag ions to form oxide particles. Given the small sizes of Ag nanoparticles (2.2 nm and 1.9 nm for PVP and SDS, respectively), a significant amount of Ag_2O can be formed on the surface. However, CTAB can only react with Ag via the brome ion to form AgBr [40]. As AgBr will be quickly reduced to Ag [41], the metallic Ag nanoparticles will react with other oxidising agents to form a thin Ag_2O layer. Therefore, a higher percentage of metallic Ag was produced when CTAB was used as surfactant material.

4. Conclusions

Ag nanoparticles were synthesised by the "pulsed plasma in liquid" technique in the presence of surfactants. Three kinds of surfactant materials (CTAB, SDS, and PVP) were added to the deionised water solution prior to synthesis to prevent nanoparticle aggregation. The effect of the surfactants on the formation of the nanoparticles was compared. PVP and SDS produced

spherically shaped silver nanoparticles with diameters of 2.2 ± 0.8 nm and 1.9 ± 0.4 nm, respectively. For CTAB, two sizes of nanoparticles with diameters of 3.2 and 17.2 nm were formed, attributed to a weak interaction between CTAB and the Ag nanoparticles. In addition, the ratio of the constituent phases, Ag and Ag_2O by weight percentages, was calculated from the integrated peak areas in XRD. The fraction of metallic Ag in the nanoparticles increased with the increase of the size of Ag nanoparticle. This study demonstrates a new route to synthesise Ag nanoparticles in a scalable way, with potential applications in biotechnology.

Author Contributions: Conceptualization, E.O., R.E.P., A.S. and Y.N.; formal analysis, Y.N., R.C. and E.O.; investigation Y.N., R.C., D.S.k. and Z.Z.; writing—original draft preparation, all authors; writing—review and editing, Y.N., E.O. and R.E.P.; supervision, E.O., A.S. and R.E.P.; project administration, E.O. and R.E.P.; funding acquisition, E.O., A.S. and R.E.P. All authors have read and agreed to the published version of the manuscript.

Funding: E.O., D.S.k., Z.Z. and A.S. are funded by the Ministry of Education and Science of the Kyrgyz Republic (project #0007670). Y.N., R.C. and R.E.P. are funded by the UK's EPSRC project of "Super-Abundant Size-Selected Cluster Technology for Nanoscale Design of Functional Materials" (Grant Reference No. EP/ K006061/2).

Institutional Review Board Statement: Not applicable.

Informed Consent Statement: Not applicable.

Data Availability Statement: The data presented in this study are available on request from the corresponding author.

Acknowledgments: We would like to thank the Ministry of Education and Science of the Kyrgyz Republic, project #0007670, and the UK's EPSRC (Grant Reference No. EP/ K006061/2).

Conflicts of Interest: The authors declare no conflict of interest.

References

1. Khan, M.; Shaik, M.R.; Adil, S.F.; Khan, S.T.; Al-Warthan, A.; Siddiqui, M.R.H.; Tahir, M.N.; Tremel, W. Plant extracts as green reductants for the synthesis of silver nanoparticles: Lessons from chemical synthesis. *Dalton Trans.* **2018**, *47*, 11988–12010. [CrossRef] [PubMed]
2. Gloag, L.; Mehdipour, M.; Chen, D.F.; Tilley, R.D.; Gooding, J.J. Advances in the application of magnetic nanoparticles for sensing. *Adv. Mater.* **2019**, *31*, 1904385. [CrossRef] [PubMed]
3. Bharat, T.C.; Mondal, S.; Gupta, H.S.; Singh, P.K.; Das, A.K. Synthesis of doped zinc oxide nanoparticles: A review. *Mater. Today-Proc.* **2019**, *11*, 767–775. [CrossRef]
4. Escalera-López, D.; Niu, Y.; Yin, J.; Cooke, K.; Rees, N.V.; Palmer, R.E. Enhancement of the Hydrogen Evolution Reaction from Ni-MoS_2 Hybrid Nanoclusters. *ACS Catal.* **2016**, *6*, 6008–6017. [CrossRef]
5. Liao, T.W.; Yadav, A.; Ferrari, P.; Niu, Y.B.; Wei, X.K.; Vernieres, J.; Hu, K.J.; Heggen, M.; Dunin-Borkowski, R.E.; Palmer, R.E.; et al. Composition-tuned Pt-skinned PtNi bimetallic clusters as highly efficient methanol dehydrogenation catalysts. *Chem. Mater.* **2019**, *31*, 10040–10048. [CrossRef]
6. Sankar, M.; He, Q.; Engel, R.V.; Sainna, M.A.; Logsdail, A.J.; Roldan, A.; Willock, D.J.; Agarwal, N.; Kiely, C.J.; Hutchings, G.J. Role of the support in gold-containing nanoparticles as heterogeneous catalysts. *Chem. Rev.* **2020**, *120*, 3890–3938. [CrossRef]
7. Tan, H.W.; An, J.; Chua, C.K.; Tran, T. Metallic nanoparticle inks for 3D printing of electronics. *Adv. Electron. Mater.* **2019**, *5*, 1800831. [CrossRef]
8. Sharma, A.; Yu, H.; Cho, I.S.; Seo, H.; Ahn, B. ZrO_2 nanoparticle embedded low silver lead free solder alloy for modern electronic devices. *Electron. Mater. Lett.* **2019**, *15*, 27–35. [CrossRef]
9. Shkir, M.; Khan, M.T.; Ashraf, I.M.; AlFaify, S.; El-Toni, A.M.; Aldalbahi, A.; Ghaithan, H.; Khan, A. Rapid microwave-assisted synthesis of Ag-doped PbS nanoparticles for optoelectronic applications. *Ceram. Int.* **2019**, *45*, 21975–21985. [CrossRef]
10. Baldini, E.; Chiodo, L.; Dominguez, A.; Palummo, M.; Moser, S.; Yazdi-Rizi, M.; Aubock, G.; Mallett, B.P.P.; Berger, H.; Magrez, A.; et al. Strongly bound excitons in anatase TiO_2 single crystals and nanoparticles. *Nat. Commun.* **2017**, *8*, 13. [CrossRef]
11. Sabela, M.; Balme, S.; Bechelany, M.; Janot, J.M.; Bisetty, K. A review of gold and silver nanoparticle-based colorimetric sensing assays. *Adv. Eng. Mater.* **2017**, *19*, 1700270. [CrossRef]
12. Galdiero, S.; Falanga, A.; Vitiello, M.; Cantisani, M.; Marra, V.; Galdiero, M. Silver nanoparticles as potential antiviral agents. *Molecules* **2011**, *16*, 8894–8918. [CrossRef] [PubMed]
13. Wang, J.X.; Li, J.H.; Guo, G.Y.; Wang, Q.J.; Tang, J.; Zhao, Y.C.; Qin, H.; Wahafu, T.; Shen, H.; Liu, X.Y.; et al. Silver-nanoparticles-modified biomaterial surface resistant to staphylococcus: New insight into the antimicrobial action of silver. *Sci. Rep.* **2016**, *6*, 1–16. [CrossRef] [PubMed]

14. Richter, A.P.; Brown, J.S.; Bharti, B.; Wang, A.; Gangwal, S.; Houck, K.; Hubal, E.A.C.; Paunov, V.N.; Stoyanov, S.D.; Velev, O.D. An environmentally benign antimicrobial nanoparticle based on a silver-infused lignin core. *Nat. Nanotechnol.* **2015**, *10*, 817–823. [CrossRef] [PubMed]
15. Duran, N.; Marcato, P.D.; De Souza, G.I.H.; Alves, O.L.; Esposito, E. Antibacterial effect of silver nanoparticles produced by fungal process on textile fabrics and their effluent treatment. *J. Biomed. Nanotechnol.* **2007**, *3*, 203–208. [CrossRef]
16. Zheng, K.Y.; Setyawati, M.I.; Leong, D.T.; Xie, J.P. Antimicrobial silver nanomaterials. *Coord. Chem. Rev.* **2018**, *357*, 1–17. [CrossRef]
17. Asoro, M.A.; Kovar, D.; Ferreira, P.J. Effect of surface carbon coating on sintering of silver nanoparticles: In situ TEM observations. *Chem. Commun.* **2014**, *50*, 4835–4838. [CrossRef]
18. Murphy, C.J. Sustainability as an emerging design criterion in nanoparticle synthesis and applications. *J. Mater. Chem.* **2008**, *18*, 2173–2176. [CrossRef]
19. Cinelli, M.; Coles, S.R.; Nadagouda, M.N.; Blaszczynski, J.; Slowinski, R.; Varma, R.S.; Kirwan, K. A green chemistry-based classification model for the synthesis of silver nanoparticles. *Green Chem.* **2015**, *17*, 2825–2839. [CrossRef]
20. Sun, Y.G. Controlled synthesis of colloidal silver nanoparticles in organic solutions: Empirical rules for nucleation engineering. *Chem. Soc. Rev.* **2013**, *42*, 2497–2511. [CrossRef]
21. Hu, Y.J.; Shi, Y.L.; Jiang, H.; Huang, G.J.; Li, C.Z. Scalable preparation of ultrathin silica-coated Ag nanoparticles for SERS application. *Acs Appl. Mater. Interfaces* **2013**, *5*, 10643–10649. [CrossRef]
22. Nadagouda, M.N.; Speth, T.F.; Varma, R.S. Microwave-assisted green synthesis of silver nanostructures. *Acc. Chem. Res.* **2011**, *44*, 469–478. [CrossRef] [PubMed]
23. Baruwati, B.; Polshettiwar, V.; Varma, R.S. Glutathione promoted expeditious green synthesis of silver nanoparticles in water using microwaves. *Green Chem.* **2009**, *11*, 926–930. [CrossRef]
24. Hebbalalu, D.; Lalley, J.; Nadagouda, M.N.; Varma, R.S. Greener techniques for the synthesis of silver nanoparticles using plant extracts, enzymes, bacteria, biodegradable polymers, and microwaves. *ACS Sustain. Chem. Eng.* **2013**, *1*, 703–712. [CrossRef]
25. Pansare, A.; Shedge, A.; Chhatre, S.; Punam Murkute, D.; Pansare, S.; Nagarkar, A.; Patil, V.; Chakrabarti, S. AgQDs employing black box synthetic strategy: Photocatalytic and biological behavior. *J. Lumin.* **2019**, *212*, 133–140. [CrossRef]
26. Iravani, S.; Korbekandi, H.; Mirmohammadi, S.V.; Zolfaghari, B. Synthesis of silver nanoparticles: Chemical, physical and biological methods. *Res. Pharm. Sci.* **2014**, *9*, 385–406.
27. Zhao, J.L.; Cao, L.; Palmer, R.E.; Nordlund, K.; Djurabekova, F. Formation and emission mechanisms of Ag nanoclusters in the Ar matrix assembly cluster source. *Phys. Rev. Mater.* **2017**, *1*, 066002. [CrossRef]
28. Mashimo, T.; Shota, T.; Yamamoto, K.; Kelgenbaeva, Z.; Ma, W.J.; Tokuda, M.; Koinuma, M.; Isobe, H.; Yoshiasa, A. Synthesis of Pd–Ru solid-solution nanoparticles by pulsed plasma in liquid method. *Rsc. Adv.* **2020**, *10*, 13232–13236. [CrossRef]
29. Sulaimankulova, S.; Mametova, A.; Abdullaeva, Z. Fusiform gold nanoparticles by pulsed plasma in liquid method. *SN Appl. Sci.* **2019**, *1*, 1427. [CrossRef]
30. Kelgenbaeva, Z.; Omurzak, E.; Takebe, S.; Sulaimankulova, S.; Abdullaeva, Z.; Iwamoto, C.; Mashimo, T. Synthesis of pure iron nanoparticles at liquid–liquid interface using pulsed plasma. *J. Nanopart. Res.* **2014**, *16*, 1–11. [CrossRef]
31. Omurzak, E.; Jasnakunov, J.; Mairykova, N.; Abdykerimova, A.; Maatkasymova, A.; Sulaimankulova, S.; Matsuda, M.; Nishida, M.; Ihara, H.; Mashimo, T. Synthesis method of nanomaterials by pulsed plasma in liquid. *J. Nanosci. Nanotechnol.* **2007**, *7*, 3157–3159. [CrossRef] [PubMed]
32. Omurzak, E.; Abdullaeva, Z.; Iwamoto, C.; Ihare, H.; Sulaimankulova, S.; Mashimo, T. Synthesis of hollow carbon nano-onions using the pulsed plasma in liquid. *J. Nanosci. Nanotechnol.* **2015**, *15*, 3703–3709. [CrossRef]
33. El-Shabasy, R.; Yosri, N.; El-Seedi, H.; Shoueir, K.; El-Kemary, M. A green synthetic approach using chili plant supported Ag/Ag_2O@P25 heterostructure with enhanced photocatalytic properties under solar irradiation. *Optik* **2019**, *192*, 162943. [CrossRef]
34. Lee, H.; Park, S.H.; Jung, S.C.; Yun, J.J.; Kim, S.J.; Kim, D.H. Preparation of nonaggregated silver nanoparticles by the liquid phase plasma reduction method. *J. Mater. Res.* **2013**, *28*, 1105–1110. [CrossRef]
35. Lopez-Miranda, A.; Lopez-Valdivieso, A.; Viramontes-Gamboa, G. Silver nanoparticles synthesis in aqueous solutions using sulfite as reducing agent and sodium dodecyl sulfate as stabilizer. *J. Nanopart. Res.* **2012**, *14*, 1–11. [CrossRef]
36. Song, K.C.; Lee, S.M.; Park, T.S.; Lee, B.S. Korean, Preparation of colloidal silver nanoparticles by chemical reduction method. *J. Chem. Eng.* **2009**, *26*, 153–155.
37. Zhang, W.Z.; Qiao, X.L.; Chen, J.G. Formation of silver nanoparticles in SDS inverse microemulsions. *Mater. Chem. Phys.* **2008**, *109*, 411–416. [CrossRef]
38. Baruah, B.; Kiambuthi, M. Facile synthesis of silver and bimetallic silver–gold nanoparticles and their applications in surface-enhanced Raman scattering. *RSC Adv.* **2014**, *4*, 64860–64870. [CrossRef]
39. Locke, B.R.; Sato, M.; Sunka, P.; Hoffmann, M.R.; Chang, J.S. Electrohydraulic discharge and nonthermal plasma for water treatment. *Ind. Eng. Chem. Res.* **2006**, *45*, 882–905. [CrossRef]
40. Jin, W.; Liang, G.; Zhong, Y.; Yuan, Y.; Jian, Z.; Wu, Z.; Zhang, W. The Influence of CTAB-capped seeds and their aging time on the morphologies of silver nanoparticles. *Nanoscale Res. Lett.* **2019**, *14*, 81. [CrossRef]
41. Zhong, Y.; Liang, G.; Jin, W.; Jian, Z.; Wu, Z.; Chen, Q.; Cai, Y.; Zhang, W. Preparation of triangular silver nanoplates by silver seeds capped with citrate-CTA+. *RSC Adv.* **2018**, *8*, 28934–28943. [CrossRef]